Chapter 2

MODEL-FREE DECONVOLUTION OF TRANSIENT SIGNALS USING GENETIC ALGORITHMS

László Bengi, Balázs Kovács, Máté Bezdek and Ernő Keszei
Eötvös University Budapest, Department of Physical Chemistry,
and Reaction Kinetics Laboratory

ABSTRACT

Model-free deconvolution of transient signals usually suffers from a wavy small-frequency component as well as an increase of high frequency noise. The more these features are damped, the more the deconvolved signal becomes distorted. If we can include as much information concerning the genuine deconvolved signal as possible, the quality of the deconvolved transient can be greatly improved.

We have developed a deconvolution procedure which does not make use of a pre-supposed (often arbitrary) functional form of the transient signal. Instead, it is based on the inversion of the distortion effects of convolution, which means temporal compression, amplitude enhancement, increasing of the steepness of rise and decay of the measured convolved signal, and cutting initial data to zero to reproduce an eventual sudden jump. As our results have proved that the choice of a fairly good initial population is crucial for a successful deconvolution, we use additional genetic algorithms to generate an initial population with a relatively high fitness.

The initial population is generated from the measured convolved signal in two subsequent stages, each consisting of a genetic algorithm and the check of the potential to improve the fitness of the population during further breeding, as a candidate for the deconvolved data set. This generation can be done "automatically" so that the user does not need to experiment much to get a good initial population and satisfactory final results.

The final genetic algorithm performing the main iteration to get the estimate of the deconvolved data is constructed in such a way that it does not enhance either the low-frequency wavy behaviour, or the high frequency noise. It is based on a smooth mutation in a range containing several data, and a dynamic adjustment of the mutation.

The method is described in connection with the deconvolution of ultrafast laser kinetic (or femtosecond chemistry) data. The advantage of this method to find an underlying molecular mechanism via statistical inference is also discussed.

Keywords: deconvolution, genetic algorithm, transient signals, femtochemistry, fluorescence decay.

1. INTRODUCTION

Deconvolution is a process to reverse the result of – usually unwanted – convolution which distorts measured signals.[1-3] In many cases, measured signals are not those we are interested in, but – due to the limited capacities of the measuring apparatus – they are distorted by a phenomenon that can be interpreted as collecting data by moving averages. If we consider a continuous time-dependent signal $o(t)$ to be measured, the effect of *convolution* means that instead of this function, we can only measure

$$i(\tau) = \int_{-\infty}^{\infty} o(t)\, s(\tau - t)\, dt \quad . \tag{1}$$

Using terms of image processing, the *measured image function* $i(\tau)$ is the integral with respect to time of the product of the true *object function* $o(t)$ and the distorting *spread function* $s(\tau - t)$. Signals are typically measured as a discrete time-series of digital recordings. The discrete equivalent of the convolution equation (1) is the sum

$$i_k = \sum_{k-M}^{k+M} o_i s_{k-i} \,, \tag{2}$$

where i_k is the k-th recording of the time-series of the image function measurements, o_i is the actual value of the object function between the recordings $k - M$ and $k + M$, and s_{k-i} is the integral of the spread function within one measured interval between $k - M$ and $k + M$. This latter equation illustrates more transparently the moving average over $2M + 1$ discrete (non-zero) values of the spread function. (We get a genuine average without dividing by the sum of all the nonzero s_{k-i} values if the spread function is defined so that the sum of its values between $k - M$ and $k + M$ is exactly unity. In this case, we can also consider the spread function as a kind of probability distribution characterizing the detection device. This is also why it is called the *instrument response function*.) As a result, the measured time series will be a distorted version of the original object function time series o_i. Integral (1) or the sum (2) is usually written in a shorthand-type notation as

$$i = o \otimes s \,, \tag{3}$$

which is fully equivalent to either of the two equations. The symbol $\otimes$ denotes the operation of convolution.

To get the true object function o from the known i and s, we have to solve the convolution equation (1) or (2). This procedure is called *deconvolution*. As we can see, the (analytical) task is to solve an integral equation; thus the operation of convolution does not

have a simple inverse. This problem can be circumvented with the help of an integral transformation. The *Fourier transform* (FT) of the image function (I) is simply the product of the Fourier transforms of the object (O) and the spread (S) functions: [3]

$$I = O \cdot S \tag{4}$$

As the product does have an inverse, it is easy to get the FT of the object function O when dividing I by S. The inverse Fourier transform then readily provides the original object function o.

If the detection of the measured signal is free of any errors, the solution can be unique. However, if the measured signal contains some error (even if it is only a rounding-off error due to digital truncation of the recorded values), we get an infinite number of solutions. This means that no unique solution exists for any measured convolved data sets, which can easily be shown if we write the additional noise term explicitly:

$$i = o \otimes s + n \ , \tag{5}$$

where n is the noise term. Due to the distributivity and associativity of convolution [3], this can be rewritten as

$$i = o \otimes s + n = o \otimes s + n' \otimes s = (o + n') \otimes s \ . \tag{6}$$

Accordingly, the convolved noisy signal is equivalent to the convolution of the sum of the true object function and the "deconvolved noise" n'. Due to the additivity, *any* function n' added to the true object will give the measured image whose convolution with the spread function results in zero. Obviously, there exist infinite such functions with a high-frequency oscillation, as such oscillations disappear when their weighted average is calculated by convolution. Solution in the frequency domain – which makes use of the simple division of the Fourier transforms – does not help either. Both the image and the spread are relatively slowly varying functions (compared to the width of the sampling intervals), thus the high-frequency components in the FT in both cases are very much close to zero. Due to experimental errors, this "zero amplitude" fluctuates quite substantially, which is further amplified by the division of the close-to-zero image FT by the close-to-zero spread FT. The resulting inverse FT – the estimate of the original object – typically contains much more noise than signal.

This is a major problem during the deconvolution of measured signals, which inevitably contain some noise. The consequence is that a simple-minded deconvolution usually results in a rather noisy deconvolved data set, along with a lower frequency wavy behavior somewhere in the dominant frequency range of the spread function. There are several methods used that get rid of these unwanted features, which are more or less efficient. Most of them are based on the fact that the noise content results in a high-frequency oscillation, thus the elimination (or at least a severe limitation) of high-frequency components avoids this oscillation. However, if there are sudden changes in the true object function – which is typically the case in transient signals –, this damping of high-frequency components leads to a distortion of the reconstructed object function. Keeping in mind that the effect of noise is a kind of artifact in

the deconvolved function, information about the true shape of the original object function helps a lot to drive the solution towards a physically sound deconvolved. The more information we can enter into the deconvolution procedure, the better estimates of the true object we can get.

In our previous research concerning ultrafast laser chemistry (or *femtochemistry*) measurements, we have tried to use deconvolution methods described in the literature. We have challenged several time-domain iterative methods, and many frequency-domain methods, including digital filtering and regularization.[4-6] We have found that proper adaptation of these methods leads to quite reasonable deconvolution results. However, none of them provide a genuine noise-free, unbiased deconvolved result, unless we know the functional form of the object function and search only for the parameters of this function so that the *reconvolved* – the calculated equivalent of the image function – best fits the measured image. However, this *reconvolution* is not a true deconvolution method; it is more of a fitting procedure that estimates the parameters of an already known function. In many physical problems, no model of the measured object is known *a priori*, thus it is necessary to calculate a *model-free* (*or nonparametric*) *deconvolution* of the measured signal. The nature of this task necessitates so called *soft methods* to search for a physically sound solution. One of the soft methods that has been found to be very effective in solving many problems is a genetic algorithm. [7] In addition to its great power to find a solution, a genetic algorithm also makes use of constraints, "herding" the solution by specifying several constraints derived from the *a priori* knowledge about the shape of the desired solution. This is the reason we have developed a method based on genetic algorithms to perform model-free deconvolution of transient signals.

Genetic algorithms are not widely used for deconvolution purposes yet, but – as it turned out from our research presented here – they are rather promising candidates to be used more widely in the near future. We have only found relatively few applications in the literature including image processing [8-10], spectroscopy [11-12], chromatography [13-15], and pharmacokinetics [16]. Most of the applications are not using model-free deconvolution but reconvolution methods, where the fit of the reconvolved model function to the measured data is performed, thus only parameters of this fit are determined using a genetic algorithm. It should also be noted that the term "deconvolution" is often used for the process of decomposing a set of overlapping peaks into separate components via curve fitting of peak models to the measured data set. This is conceptually distinct from deconvolution, because in deconvolution the original peak shape is unknown, and the measured function is distorted by the spread function. In the decomposition procedure, there is no distortion of the composite peak resulting from the superposition of the components, only a resolution of the components is necessary.

In this chapter we describe the use of genetic algorithms (GAs) that we successfully implemented for model-free (nonparametric) deconvolution of a special kind of transient signals: femtosecond kinetic traces. We do not deal with blind deconvolution where only the image is known and both the spread and the object are determined during the deconvolution procedure; only with deconvolution in case of known image and spread. After a brief description of the physical background concerning unwanted and unavoidable convolution in femtochemistry experiments, we describe synthetic functions to test deconvolution. The main part of the chapter deals with the description of the particular genetic algorithm used to estimate the deconvolved data set. This also includes a careful selection of the initial

population, which is automatically generated using two subsequent steps also based on genetic algorithms. Following the discussion of the performance of this procedure tested on synthetic images, we also show deconvolution of real-life experimental data. The chapter ends with a conclusion, discussing an outlook to use the described deconvolution procedure for other problems where convolved transient signals occur.

2. CONVOLUTION OF THE MEASURED SIGNALS IN FEMTOCHEMISTRY

Femtochemistry is a new branch of molecular science dealing with direct experimental observation of molecular events during the breaking of chemical bonds and the formation of new bonds. [17-18] These events typically happen at timescales ranging from a few tens to a few hundreds of femtoseconds (fs), *i. e.*, between about 20×10^{-15} and 500×10^{-15} seconds. As the clocking speed of any available electronic devices is several orders of magnitudes lower, real-time measurements cannot be made at this timescale. To circumvent this limitation, the speed of light is used for clocking. First, an ultrashort laser pulse excites the molecules and thus starts the reaction, followed by a second laser pulse that tests some optical properties of the reacting system. The reaction time is coded into the delay between the two pulses. As 1 μm difference in the optical path length is equivalent to roughly 3 fs delay, a mechanical or electromechanical device is convenient to control the path length so that 1 fs delays can be adjusted easily.

Ultrafast laser pulses can be as short as 10 fs. However, excitation and detection are expected to be selective, which necessitates that their spectral width be quite small. Due to the uncertainty relation between time and energy, the typical pulse width is usually limited to about 100 fs or more.[19] Thus, characteristic times to be measured are about the same as the width of the laser pulses used to measure them; which results in convolved measured signals. A detailed description of how the convolved signal emerges is given elsewhere.[7] Here we only recall the result: the detected signal is a convolution of the *effective pulse* (spread, or the instrument response function, which is the correlation of the exciting and measuring pulses) and the *object*, as given in Eq. (3). As a consequence, femtosecond kinetic traces are usually heavily distorted by the convolution described above. Consequently, it is necessary to deconvolve femtochemical transient signals when performing a kinetic interpretation of the observed data. Typical data sets can be seen in Figures 4-6.

3. DECONVOLUTION USING GENETIC ALGORITHMS

In the "classical" version of a GA, individuals are represented as a binary string, which codes either the complete solution, or parameters to be optimized. These strings are considered the genetic material of individuals, or *chromosomes*, while the bits of each string are regarded as *genes*, having two different *alleles*, 0 or 1. It is often problematic to represent a solution in the form of binary strings. Thus, for numerical optimization purposes, *floating point* coding is more convenient, which allows for a virtually infinite number of alleles. Classical (binary) genetic operators have also been replaced accordingly by *arithmetic* operators. The "art" of using GAs is in finding a suitable representation or data structure for

the solution, and using genetic operators that can explore the *solution space* in an efficient way, avoiding local optima and converging quickly to the global optimum. [20-21]

Deconvolution methods described in the literature use different representations and a variety of genetic operators. While binary coding and classical binary crossover and mutation are appropriate for processing black and white images [9-10], quite different encoding and operators should be used to deconvolve measured kinetic signals.[21] Generation of the initial population may also be critical. One method is the completely random generation of the first individuals, while a careful generation of already fit individuals is sometimes important.

When deconvolving femtosecond kinetic data using GAs, potential problems that may arise are similar to those of other methods: we should avoid the amplification of experimental noise and the oversmoothing of the image that results in – among other effects – a low frequency "wavy" distortion. The non-periodic nature and sudden stepwise changes of the transient signals should also be reconstructed without distortion. We have found that the above needs cannot be fulfilled if we start the GA with a randomly generated initial population. Therefore, the first task is to create individuals who already display some useful properties of a good solution.

3.1. Data Structure

The solution of the convolution equation (2) is a data set containing the undistorted object (instantaneous kinetic response) at the same time instants as the measured image function. Conveniently, the coded solution is this data set, which is an array containing floating point elements, with each element representing a measured value of the undistorted object. In terms of GAs, this is a single haploid chromosome containing as many genes as there are data points measured. As each parent and each offspring is a haploid, there is a haploid mechanism of reproduction to implement, in which two parent chromosomes are combined to form a single haploid chromosome of the offspring. There is no need to "express" the genes as phenotypes; the chromosome already represents the solution itself.

Convolution – since it is a kind of weighted moving average – *widens* the signal temporally, *diminishes its amplitude*, makes its *rise and descent less steep*, and *smoothes out* its sudden steplike jumps. Accordingly, to create a fairly fit initial population, we started from the image itself and implemented an operator to *compress* the image temporally, another to *enhance its amplitude*, third and fourth ones to *steepen its rise and decay*, and finally, a fifth operator to *restitute the stepwise jump* by setting some leading elements of the data to zero. All five operators – which we may call *creation operators* – are constructed to conduct a random search in a prescribed modification range. To this purpose, normally distributed random numbers are generated with given expectation and standard deviation for the factor of temporal compression, of the enhancement of amplitude, for increasing the steepness of rise and decay, and for the number of data points to be cut to zero at the leading edge of the data set. The effect of these operators is schematically represented in Figure 1.

The first implementation of the GA for deconvolution started with a user-defined set of creation operators, and the resulting initial population was displayed graphically, along with the original image. The best individual of this population and the result of the convolution of this individual with the spread function (the *reconvolved*), as well as the deviation of this reconvolved from the image were also displayed.

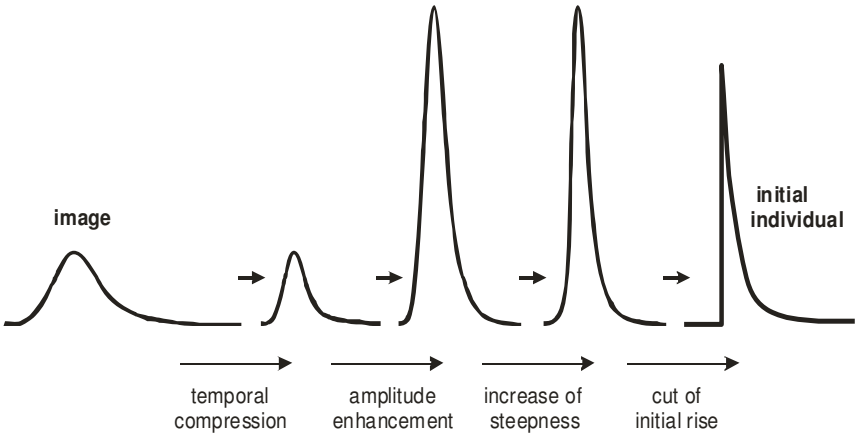

Figure 1. Schematic representation of the creation of initial individuals from the measured image function. The four steps depicted here show the effects of five different creation operators applied subsequently.

If the user found that the reconvolved data set was too different from the image, or if there were spurious oscillations present in the best individual, the user initiated another selection of the initial population with different expectation and/or standard deviation parameters of the creation operators. The procedure was repeated until the user considered the selected initial population satisfactory.

In order to arrive at fairly good estimates of the deconvolved data set that contained no spurious oscillations and had the desired shape, this trial and error procedure of finding satisfactory creation operators required somewhat tedious experimentation. The procedure also required good insight on the part of the user, not only in the details of the kinetic background involved, but also in the way the procedure responded to changes in the creation parameters. This was the reason that motivated the development of another method, also based on genetic algorithms, to replace user experimentation, which is explained following the description of the applied breeding procedure.

3.2. Parent Selection and Crossover

The quality of the deconvolved data set – an individual of the population – can be measured readily by the mean square error (*MSE*) of the reconvolution, given by

$$MSE = \sqrt{\frac{\sum_{k=1}^{N}\left[\left(\hat{o} \otimes s\right)_k - i_k\right]^2}{N-1}}\ , \tag{7}$$

where $\hat{o}$ is the estimate of the deconvolved, *i. e.*, the actual individual of the population, and N is the number of data in the image data set. GA literature suggests that some kind of *inverse* of this error should be used so that the resulting fitness function is normalized. We

implemented a dynamic scaling of fitness by adding the minimal *MSE* of the population in the denominator:

$$fitness_j = \frac{1}{\min(MSE) + MSE_j}, \tag{8}$$

which maintains the fitness values in the range from 1 / [min(*MSE*) + max(*MSE*)] to 1 / [2 min(*MSE*)].

To choose parents for mating, we use stochastic sampling with replacement, implemented as a *roulette-wheel selection*. [20-21] Offsprings are produced by *arithmetic crossover* of the parents, resulting in an offspring whose data points are the average of the parents' data. (Fitness-weighted averages did not result in an important difference concerning convergence and the quality of the winner.) This procedure of parent selection and crossover is made until the number of produced offspring becomes the same as in the previous population.

3.3. Mutation and Selection of the New Generation

Arithmetic crossover explores the potential solutions solely within the range represented by the initial population; it cannot drive the population out of this region. Mutation is therefore needed to further explore the fitness landscape of the solution space. In addition, a properly chosen mutation operator can also be used to avoid the usual noise amplification and low-frequency wavy behavior. A brute-force mutation by randomly changing the values of individual data points has the consequence of increasing the noise content of the signal, as reconvolution prior to the computation of fitness smoothes out even large differences in neighboring points, thus the population would evolve to a better fit by increasing high-frequency noise. In contrast, a "smooth" mutation of neighboring data points results in an effective smoothing of the mutated individuals after a few crossovers. It has been implemented as an addition of a randomly generated Gaussian to the actual data set. The expectation (centre), the standard deviation (width) and the amplitude of the additive Gaussian correction is randomly selected within a specified range, including both positive and negative amplitudes. (Leading zeros of the initial population get never changed by mutation, which is equivalent to a semi-finite-support constraint. [1,6]) If the kinetic response function has a long tail (*e. g.* due to largely different characteristic times involved in the reaction mechanism), its slow decrease can also be reconstructed by this mutation, even if the initial population had a much sharper decrease without a long tail.

There is another feature which proved to be useful in finding the fittest possible individuals; non-uniform mutation. [20] This is responsible for fine-tuning the mutations in such a way that it drives even a rather uniform and close to optimal population further towards the global optimum. If the mutation amplitude is small, the convergence at the start of the iteration is also small. A larger amplitude results in a faster convergence but makes the improvement of individuals quite improbable after the deviation of the solution from the optimum is much less than the mutation amplitude, as mutations typically result in a less fit individual compared to the one prior to mutation. To effectively get closer to the optimum, it is necessary to diminish the amplitude of the mutation as the number of generations increases,

or with decreasing deviation from the optimum. We perform this adjustment by estimating the experimental error as the standard deviation of measured image data in the range where its values are more or less constant. (*E. g.*, in the leading zero level of the signal, or in an almost constant tail.) Comparing this experimental error to the difference between the *MSE* of the fittest and the least fit individuals, the amplitude parameter of the Gaussian mutation is multiplied by the factor

$$f = 1 - e^{1 - \left(\frac{MSE \text{ difference}}{\text{experimental error}} \right)^p} . \tag{9}$$

The factor f approaches zero as the ratio of the *MSE* difference between the most and least fit individuals to the experimental error approaches one. This correction avoids too large modifications, thus resulting also in a less noisy deconvolved data set. The higher the power p, the more enhanced the tuning effect of the factor. A value of the exponent $p = 1.5$ proved to be efficient when deconvolving the data shown in this chapter. To avoid problems arising from a possible overestimation of the experimental error, the factor f can be checked and set equal to a prescribed smallest value if the ratio in the exponent is too close to one, or even less.

When the number of newly generated offsprings equals the population number minus one, selection of the new generation is done. All the parents die out except for the fittest one, which also becomes member of the next generation. This selection method is called *single elitism* and guarantees a monotonous improvement of the best individual.

3.4. Termination and the Choice of the Winner

After each generation, the quality of individuals is evaluated by the *MSE* between the image and the reconvolved, as this quantity is used to calculate the fitness. In addition, the differences between the reconvolved fittest individual (the *winner*) and the image – the residual errors – are calculated. For this residual data set, Durbin-Watson (DW) statistics indicate whether subsequent differences are correlated – pointing to systematic error. [22-23] The equivalent of the experimental error – the standard deviation of a few data points of the image data set, which can be considered constant – can be calculated similarly from the deconvolved data.

As a termination criterion, we can check if the *MSE* between the image and the reconvolved set of the winner is less than or equal to the experimental error. However, this does not guarantee that the reconvolved solution closely matches the image; there might be some bias present in the form of low-frequency waviness. It is the Durbin-Watson statistics that sensitively indicates such misfits. For the large number of data in a kinetic trace (typically more than 200), its critical value for a test of random differences is around 2.0 [22-23], and it is typically much lower than that for a wavy set of differences. Thus we may either use a DW value close to 2.0 as a criterion, or combine the experimental error criterion with the DW criterion so that both of them should be fulfilled.

There are less specific GA properties that can also be used to stop the iteration. If the *MSE* of the best individual does not change for a prescribed number of generations, the

algorithm might have converged. Similarly, if the difference between the *MSE* of the best fit and the least fit individual becomes less than the experimental error, we cannot expect too much change in the population due to mutations. However, the use of these criteria only indicates that the GA itself has converged but it does not guarantee a satisfactory solution.

3.5. Automatic Generation of a Fairly Good Initial Population

Having explained the breeding procedure of the genetic algorithm, let us return to the problem of creating a fairly good initial population which can evolve to give a physically sound deconvolved data set, having all the properties the user expects. The first step of the creation is to get an estimate of the deconvolved signal by using inverse filtering. We use a modified adaptive Wiener filter for this purpose. [4,6] This filtering usually results in a wavy and somewhat noisy deconvolved data set, but its onset – the first nonzero data point – can be approximately calculated in the following way. The data point between the first nonzero value and the maximum of the Wiener-filtered deconvolved is determined. The onset of the object function is in the vicinity of this location. To explore the fitness landscape, typically 50 individuals are created at each location within the range, considering it as the actual onset. Values of the other creation parameters are also generated with a uniform probability distribution, except for the maximum enhancement of the signal which is the same for all individuals. The fittest initial individual is chosen from all the initial populations, and the location of its onset will become the next estimate of the onset of the object function.

The procedure then continues in a second stage with the creation of other initial generations, this time within a narrowed range of equally distributed onsets of the individuals around the new location. Values of the other creation parameters are now generated with a normal distribution using their expectation and standard deviation given in the project description file. Breeding is done usually for 50 generations in this stage. (This number can, of course, be different.) However, the search in this stage is not for the fittest individual within a generation, but for the initial population in which the fitness increases most, compared to that of the fittest individual at the end of the first stage, as it has the greatest potential to improve. To determine this, each initial generation is bred several times (we typically use 20 breedings) with a different series of random numbers. After each of the 20 different breeding runs, the one that contained the fittest individual is noted. The “winner of the creation” will be the population that proved to increase in fitness most, with respect to the fittest individual at the end of the first stage, most frequently out of the 20 breedings. Its location of the onset and the rate of enhancement of amplitude will be used to generate the initial population of the final genetic algorithm to search for the optimal deconvolved data set.

In some cases – when the transient signal does not have a steplike onset but a slower rise – the two stages described above do not always give a satisfactory result. They often miss the true onset of the object function (which is known for synthetic data) by a few data points. However, the user is able to see the mismatch and can manually correct for the onset which gives the best result visually. Therefore, there is also a possibility to fix the location of the onset, in which case the first two stages are skipped and the procedure begins with the third stage by creating an initial population using the input values of the creation parameters.

3.6. Implementation of the Deconvolution Procedure

We have implemented the procedure described above as a package of user defined Matlab functions and scripts. The control of the deconvolution procedure is done by a graphical user interface (GUI). All the input data including filenames and operator parameters can be entered via this interface. As these data are then all written into a project descriptor text file, there is also a possibility to simply enter the name of a previously saved project descriptor file to reload all its data. The output file contains the entire project descriptor, statistical evaluations, and all relevant results. In addition, there is a four-panel figure displayed, containing most of the results for immediate graphical evaluation after each stage of the procedure.

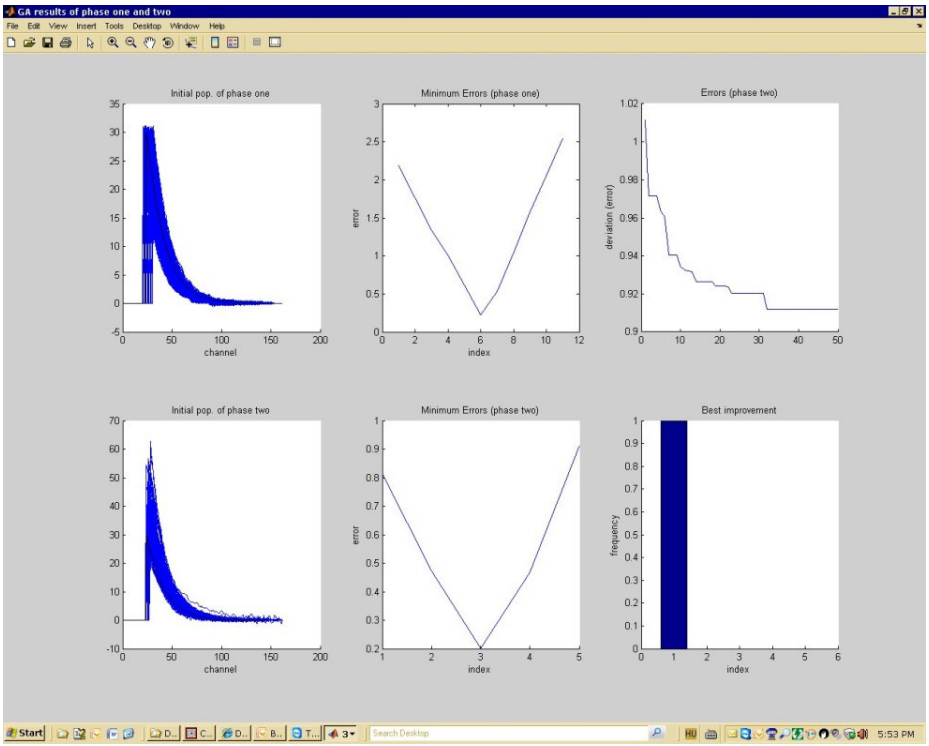

Figure 2. Screenshot after the first two stages searching for a fairly good initial population. For the description of the panels, see text.

In case the value of the input parameter specifying the expectation of the location of the first nonzero element is zero, the procedure starts with the first two stages searching for the location of the onset of the deconvolved signal. At the end of this procedure, the results of the two stages are displayed graphically in a six-panel figure (see Figure 2). The upper left panel shows the initial population generated with onsets around the location obtained with Wiener filtering. The upper middle panel is the most important here; it shows the MSE errors of the best individuals at each location after the first breeding stage, as a function of the channel index. As we can see, in Figure 2 it is channel No. 6 which gives the fittest individual. The upper right panel shows the evolution of the MSE errors of the fittest individual in each

generation as a function of the number of iteration steps (*i. e.* the number of subsequent generations). In the figure we can see that an improvement of fitness (decrease of the MSE error) occurred until step No. 32, but there was no improvement from then up to step No. 50.

The lower left panel shows the initial population generated with onsets around the location obtained as that of the fittest individual at the end of the first stage. It is clearly seen that the variety of the individuals in this population is greater than in the first stage, but in a narrower interval of the location of the onset (five channels instead of twelve). The lower middle panel shows again the *MSE* of the best individuals at each location after the second breeding stage, as a function of the channel index. However, this time it is not this statistics that is used to choose the winner, but the frequency at which an initial population becomes the fittest one after 20 breedings with different sets of random numbers to control the procedure of generating the initial population as well as the breeding procedure, which is shown in the lower right panel. In this particular case, it is the initial population generated with the onset at channel No. 1 which has the greatest improvement 20 times out of the 20 runs, thus it had been chosen as the winner. (If there are more than one placements of the onset resulting in a few best scores, it is the one with the highest frequency which is chosen as the winner.) The winner of this second stage determines the placement of the onset, and this value is used as the expectation of this parameter to generate the initial population used in the "main" GA to search for the optimal deconvolved data set.

After the first two stages, the user can observe the graphically displayed results described above, and can decide whether to launch the main GA, or halt the procedure and restart with a different set of creation parameters. If the decision is to continue the procedure, the number of iteration steps (the number of subsequent generations) can be determined before actually launching the main iteration.

In case the value of the input parameter specifying the expectation of the location of the first nonzero element at the beginning of the procedure is different from zero, the procedure skips the first two stages and uses the location of the onset of the deconvolved signal entered to generate the initial population for the main GA iteration.

At the end of the prescribed number of iterations, the program halts and a four-panel figure is displayed (see Figure 3). The upper left panel shows the image (measured) data set, the spread function (called "pulse" in the figure), the object function in case of a synthetic data set (in which case the object is known), along with the initial population. The upper right panel shows the evolution of the *MSE* of the best individual in subsequent generations, as a function of the iteration number (or generation number). The lower left panel shows the results; *i. e.* the deconvolved data set (the "winner"), its reconvolved with the spread function, along with the original image for comparison. In the case of synthetic data, the object function is also shown for comparison with the deconvolved result. (In the figure, due to the screen resolution, the differences between the image and reconvolved, as well as the differences between the object and winner cannot be seen.) The lower right panel helps to judge the nature of differences between the data sets shown in the lower left panel by displaying their (discrete) Fourier transforms. These transforms show the frequency behavior of the corresponsing time series, which sensitively detect mismatches and contain useful information on the success of the deconvolution. We do not deal with the details of the Fourier transforms here; the interested reader is advised to consult an earlier publication. [5] If the user is content with the final results, the procedure is finished. If the results are not

satisfactory, a new run with or without the first two stages can be made, starting with a different set of input parameters.

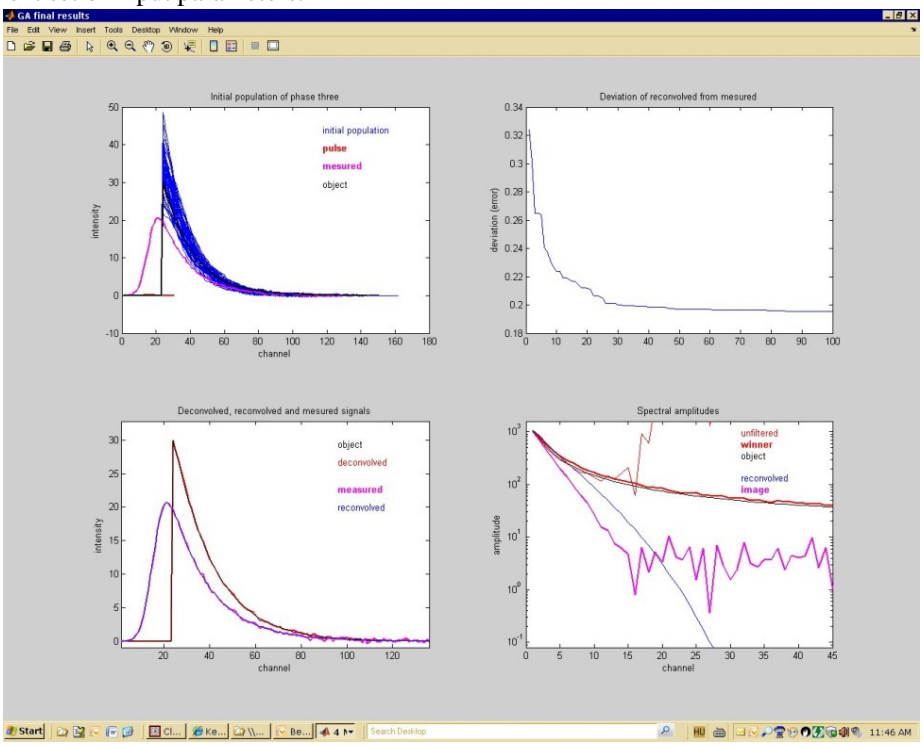

Figure 3. Screenshot showing the graphical display of the final results of deconvolution, after the main iteration. For the description of the panels, see text.

4. RESULTS

To test the performance of the algorithm, we used synthetic data calculated for a simple consecutive reaction containing two first-order steps; the first with a 200 fs, the second with a 500 fs characteristic time, as described in previous publications. [4-6] They mimic different typical transient absorbance signals. The first one is recorded at a wavelength where a completely decomposing reactant species can be detected with no remaining absorptivity ("reactant"), the second one at another wavelength with an absorbing intermediate species and also a product with positive remaining absorptivity, while the third one is similar but with a negative remaining absorptivity ("bleaching"). Calculated object data have been convolved with a 255 fs fwhm Gaussian spread function, and an "experimental noise" of 2 % of the maximum of the signals was added to the convolved data set to become the model of measured data. As recent measurements in fluorescence detection explored extremely short characteristic times with simultaneous long-time components [24-25], we also tested a fourth synthetic data set mimicking this situation, with time constants of 100 and 500 fs, and a spread function of 310 fs fwhm. While the absorption data set with bleaching necessitates the most careful transformations using the creation operators, the fluorescence decay challenges

the power of the algorithm to reconstruct an extremely large stepwise jump followed immediately by a steep decay and ending in a long tail.

4.1. Test Results for Synthetic Data

Figure 3 shows the best result obtained for the reactant transient absorption signal. As it can be seen, there is no visible difference between the deconvolved set and the synthetic object data, except for the "experimental error" added to the synthetic image. However, fluctuations in the deconvolved data set are inferior to that of the image data set which means that an effective smoothing of the "experimental errors" has also been achieved by the genetic algorithm performing deconvolution. Due to the creation operator that renders the leading data prior to the onset of the signal to zero, the steplike jump of the signal is completely reproduced, without any wavy behavior. (Leading zero values are not modified by mutations either.) Thus, we can conclude that a transient with a sudden jump and fast decay that undergoes a severe distortion due to convolution can be deconvolved to an unprecedented level.

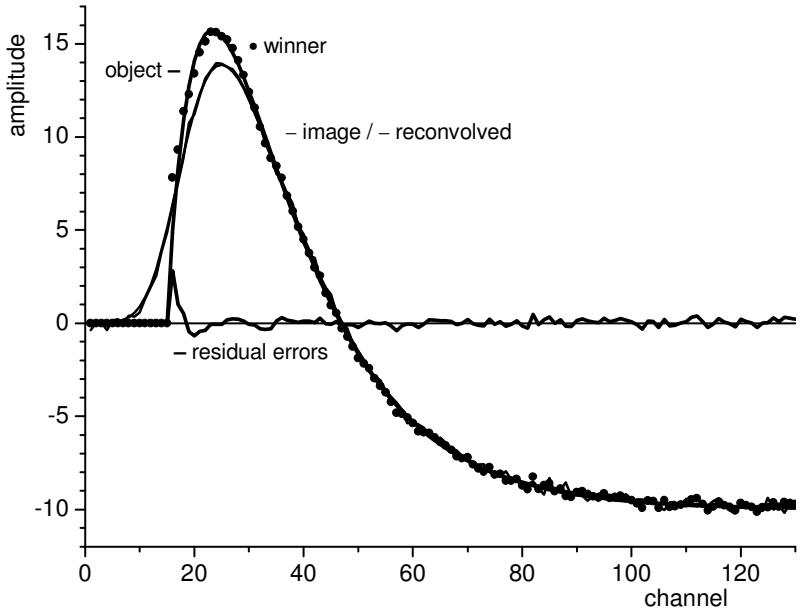

Figure 4. Deconvolution results for a non-periodic transient signal with a negative final level (in femtochemistry, it is an intermediate absorbing species with a residual bleaching). The two smoothly rising overlapping curves (solid lines) show the initial image data set to be deconvolved, and the final estimate of the deconvolved signal reconvolved with the spread function (labelled as reconvolved). The solid curve with a sudden jumplike rise is the object function without errors. Closed circles indicate the values obtained for the deconvolved at the end of the final iteration (labelled as winner). Residual errors are shown as a solid curve around zero signal level, calculated as the difference between the winner and the object.

Figure 4 shows the results obtained for the transient signal with bleaching. This signal is not periodic, as its initial value is not identical to the last one; there is a large difference between the first and last data points. In the context of the genetic algorithms used, this

problem can be treated with a careful design of the creation operators in a way that the beginning and the end of the data set should not change while applying the changes schematically illustrated in Figure 1. The success of this procedure can be illustrated by the final result of the deconvolution, shown in Figure 4. The matching smooth continuous curves are again the "measured" image and the reconvolved data set, which can hardly be distinguished at the resolution of the figure. The object (continuous curve with a steplike rise) is almost completely fit by the winner of the GA iteration (circles). Residual errors are displayed as another continuous curve close to zero signal level, which indicate a randomly distributed small fluctuation of the winner around the true object, except for a few initial points following the onset of the signal. However, this initial part of the signal is always very hard to reproduce by deconvolution; it contains typically a few initial mismatches in a wavy form. This initial wavy bias is usually present even in the case of reconvolution using a known model function.

It should also be added that the deconvolution procedure described in this chapter has been primarily optimized to the steplike transient function (reactant-like absorptivity or fluorescence decay). To illustrate the success of this optimization, deconvolution results for the simulation of the highly distorted fluorescence signal mentioned above are also shown in Figure 5. The notation of this figure is similar to that of Figure 4, with the matching "measured" and reconvolved data sets, the object and the winner, along with the residual errors concerning these latter data. The challenge of deconvolution in this case is to reconstruct the large maximum of the steplike jump which is more than four times the maximum of the image, and the long tail which begins with a much steeper decay than the image, and goes over into a shallower final part than the image. As we can see from the residual errors, there are no marked wavy mismatches at the very beginning of the signal, thus the maximum is also excellently recovered by the deconvolution.

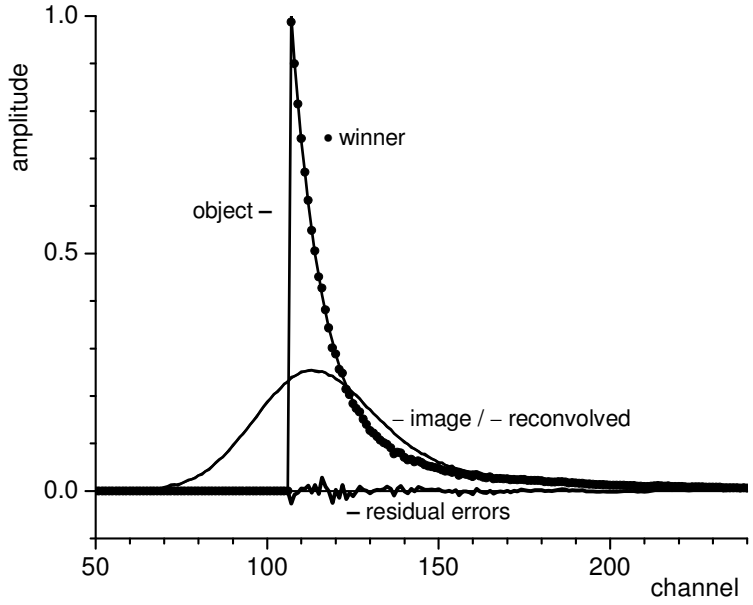

Figure 5. Deconvolution results for a heavily distorted reactant signal with a sudden initial jump followed by a steep decrease and ending in a rather shallow tail (in femtochemistry, it can be a reactant-

like absorption signal, or a fluorescence decay). The description of the signals and the notation used is the same as in Figure 4.

An interesting feature of the procedure applied has been explored during the deconvolution of this transient signal. While the success of the deconvolution depends largely on a fairly close value of the signal maximum to that of the true object of the initial population, even a quite large mismatch in the tail part can successfully be eliminated during the final iteration. This is a much desired property of the procedure used if we want to deconvolve signals with largely different decay time constants. As this feature is discussed in a previous paper [7], we do not deal with it in details here.

We have also conducted another test of the deconvolution procedure. Using the best deconvolved of the three synthetic data sets calculated for a simple consecutive reaction containing two first-order steps, determined with the described procedure, we have made a global estimation of the kinetic and photophysical parameters involved. (For the description of the model function and the global estimation, see ref. 7.) The results indicate that most of the parameters have a narrower confidence interval and a smaller (or nonexistent) bias than in the case of parameter estimation from the results of a reconvolution procedure. These results support that the procedure using GAs described here leads to deconvolved data sets whose analysis provides parameters that are less correlated with each other, and are thus also less biased. However, we consider these results only preliminary, for the deconvolution of the product species with a small transitory peak and a remaining positive absorptivity is not yet satisfactory. (As it is mentioned above, optimization of the deconvolution procedure focused on the reactant-like data set.).

4.2. Test Results for Experimental Data

Model-free deconvolution is necessary if we do not know even the functional form of the object function, only some of the qualitative properties concerning its expected shape. In a real-life experiment, the image and the spread functions are only known as measured data sets. Therefore, we cannot use the comparison of the object and the winner to monitor the development and the success of the iteration procedure. (For the same reason, it has not been used either as a criterion when testing the procedure with synthetic data.) In Figure 6, we show deconvolution results of a recent experiment still unpublished, where the fluorescence decay of adenosine monophosphate in aqueous solution was measured by femtosecond fluorescence upconversion (excited at 267 nm, observed at 310 nm).

Data are collected at 33.33 fs intervals per channel, and the experimentally determined effective pulse has a width of 270 fs fwhm, *i. e.*, 8 channels. [26] As we can see, the sudden jump characteristic of fluorescence data is completely recovered by deconvolution. Residual errors (the difference between the image and the reconvolved data sets) show an almost completely random distribution with no markedly wavy feature. Fluctuations of the residual error do not exceed the experimental noise contained in the measured image. The only seemingly systematic behavior can be seen between channels 31 and 36, where there is a humplike feature in the residual error. Observing the measured image, we can state that there is a marked shoulderlike feature in this data set as well, indicating that the deconvolution procedure truly reconstructs the behavior of the measured data. Though it might be an artifact,

it might also be a kinetic effect. It is up to the user to take it seriously as an effect, or consider it an erroneous result. Apart from this small feature, the deconvolved curve has all the properties we expect from an instantaneous fluorescence response, thus we can consider the deconvolution highly successful.

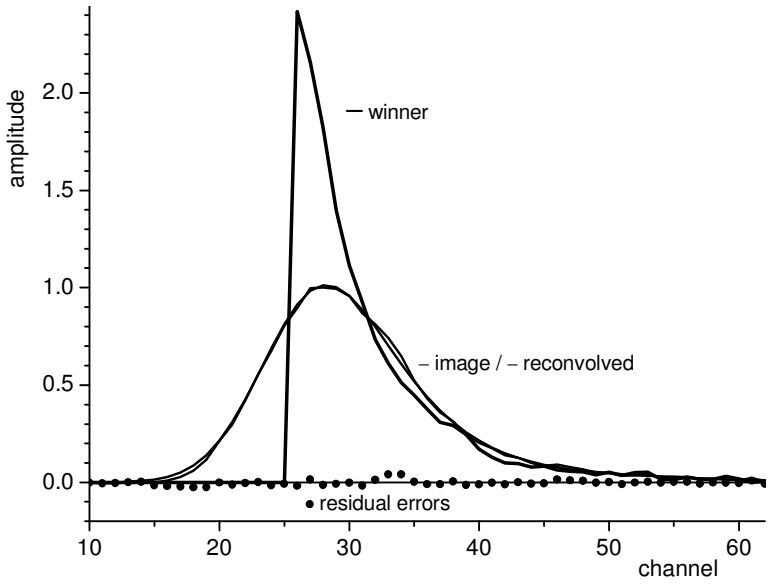

Figure 6. Deconvolution results for experimental transient fluorescence data. The two smoothly rising overlapping curves (thinner solid lines) show the initial image data set to be deconvolved, and the final estimate of the deconvolved signal reconvolved with the spread function (labelled as reconvolved). The solid curve with a sudden jumplike rise is the deconvolved data set at the end of the final iteration (labelled as winner). Residual errors (solid circles) are calculated as differences between the image and the reconvolved data sets.

CONCLUSION

Model-free deconvolution methods previously used to treat femtosecond transient kinetic data had two major shortcomings. Due to noise suppression, they resulted in deconvolved signals having a low-frequency wavy behavior, and the greater the noise suppression was, the more biased the overall shape of the reconstructed signal became. To overcome these shortcomings, we used GAs to achieve better deconvolution results. In order to adapt GAs for the purpose of deconvolving time-dependent transient signals heavily distorted by convolution, we have modified the classical GA and introduced a careful generation of the initial population and a special mutation changing neighbouring genes simultaneously.

Modification of the data structure included the use of floating-point arrays as chromosomes, representing the solution of the deconvolution problem at the chromosome level. Accordingly, genetic operators performed floating point arithmetical operations, not binary ones. To create a fairly good approximation of the deconvolved data set, we have transformed the measured image function to invert the effects of convolution. Due mainly to the operator which cuts a series of leading data of the signal to zero, and to the mutation

procedure that maintains these leading zeros, the high-frequency part of transient signals with a sudden jump-like start can be fully reconstructed. Waviness of the solution is avoided by applying smooth arithmetic mutation of neighboring genes instead of single point mutations, along with a dynamically changing mutation that fine-tunes the amplitude of the changes according to the closeness of the population to the optimal solution.

Deconvolution using this modified GA outperforms existing algorithms and produces an unprecedented quality of the reconstructed original signal for highly nonperiodic transient absorption as well as highly distorted fluorescence decay traces with a sudden initial steplike rise. Results on real-life experimental data also support the applicability of the proposed deconvolution method. Even if a few thousand generations are needed to reach an optimal solution, the iterations only take a couple of minutes on a moderately fast desktop PC. Further work is in progress to explore the full power of the applied genetic algorithm, and to develop an optimized procedure also for transients with a less sharp initial rise.

It should be noted that deconvolution is a necessary tool in many applications where it is only possible to measure a convolved signal, independently from the actual timescale of the measurement. Examples are, among others, pharmacokinetic recordings at a few hours' timescale, or transient electric signals of common devices at a few microseconds' timescale.

ACKNOWLEDGEMENTS

Thanks are due to Thomas Gustavsson and Ákos Bányász for experimental data and detailed information of the experimental conditions. Péter Pataki is acknowledged for his contribution to the Matlab code.

REFERENCES

[1] Jansson PA (editor). Deconvolution of Images and Spectra, 2nd edition; Academic Press: San Diego, 1997.

[2] A. Meister: *Deconvolution problems in nonparametric statistics*, 2009 Springer, Berlin Heidelberg.

[3] Press WH, Flannary BP, Teukolsky SA, Vetterling WT. Numerical Recipees – The Art of Scientific Computing; Cambridge University Press: Cambridge, 1986.

[4] Bányász Á, Mátyus E, Keszei E. Deconvolution of ultrafast kinetic data with inverse filtering. Radiat. Phys. Chem. 2005; 72: 235-242.

[5] Bányász Á, Dancs G, Keszei E. Optimisation of digital noise filtering in the deconvolution of ultrafast kinetic data. Radiat. Phys. Chem. 2005; 74: 139-145.

[6] Bányász Á, Keszei E. Nonparametric deconvolution of femtosecond kinetic data. J. Phys. Chem. A 2006; 110: 6192-6207.

[7] Keszei E. Efficient model-free deconvolution of measured femtosecond kinetic data using genetic algorithm, *J. Chemometrics*, 23, 188-196 (2009).

[8] Johnson EG, Abushagur MAG. Image deconvolution using a micro genetic algorithm. Opt. Commun. 1997; 140: 6-10.

[9] Chen YW, Nakao Z, Arakaki K, Tamura S. Blind deconvolution based on genetic algorithms. IEICE T. Fund. Elect. 1997; E80A: 2603-2607.

[10] Yin HJ, Hussain I. Independent component analysis and nongaussianity for blind image deconvolution and deblurring. *Integr. Comput-Aid E.* 2008; 15: 219-228.

[11] Sprzechak P, Moravski RZ. Calibration of a spectrometer using a genetic algorithm. *IEEE T. Instrum. Meas.* 2000; 49: 449-454.

[12] Tripathy SP, Sunil C, Nandy M, Sarkar PK, Sharma DN, Mukherjee B. Activation foils unfolding for neutron spectrometry: Comparison of different deconvolution methods. *Nucl. Instrum. Meth. A.* 2007; 583: 421-425.

[13] Vivo-Truyols G, Torres-Lapasio JR, Garrido-Frenich A, Garcia-Alvarez-Coque MC. A hybrid genetic algorithm with local search I. Discrete variables: optimisation of complementary mobile phases. *Chemometr. Intell. Lab.* 2001; 59: 89-106; *ibid.* A hybrid genetic algorithm with local search II. Continuous variables: multibatch peak deconvolution. *Chemometr. Intell. Lab.* 2001; 59: 107-120.

[14] Wasim M, Brereton RG. Hard modeling methods for the curve resolution of data from liquid chromatography with a diode array detector and on-flow liquid chromatography with nuclear magnetic resonance. *J. Chem. Inf. Model.* 2004; 46: 1143-1153.

[15] Mico-Tormos A, Collado-Soriano C, Torres-Lapasio JR, Simo-Alfonso E, Ramis-Ramos G. Determination of fatty alcohol ethoxylates by derivatisation with maleic anhydride followed by liquid chromatography with UV-vis detection. *J. Chromatogr.* 2008; 1180: 32-41.

[16] Madden FN, Godfrey KR, Chappell MJ, Hovorka R, Bates RA. A comparison of six deconvolution techniques. *J. Pharmacokinet. Biop.* 1996; 24: 283-299.

[17] Zewail AH, Laser femtochemistry. *Science* 1988; 242: 1645-1653.

[18] Simon JD (editor): *Ultrafast Dynamics of Chemical Systems*, Kluwer Academic Publishers, Dordrecht (1994).

[19] Donoho DL, Stark PB. Uncertainty principle and signal recovery. SIAM J. Appl. Math. 1989; 49: 906-931.

[20] Michalewicz Z. *Genetic Algorithms + Data Structures = Evolution Programs*. Springer: Berlin, 1992.

[21] Mitchell M. *An Introduction to Genetic Algorithms*. MIT Press: Cambridge, Mass., 1996.

[22] Durbin J, Watson GS. Testing for serial correlation in least squares regression I. *Biometrika* 1950; 37: 409-428.

[23] Durbin J, Watson GS. Testing for serial correlation in least squares regression II. *Biometrika* 1950; 38: 159-178.

[24] Bányász Á, Gustavsson T, Keszei E, Improta R, Markovitsi D. Effect of amino substitution on the excited state dynamics of uracil, *Photoch. Photobio. Sci.* 2008; 7: 765-768.

[25] Gustavsson T, Bányász Á, Lazzarotto E Markovitsi D, Scalmani G, Frisch MJ, Barone V, Improta R. Singlet Excited-State Behavior of Uracil and Thymine in Aqueous Solution: A Combined Experimental and Computational Study of 11 Uracil Derivatives, *J. Am. Chem. Soc.* 2006; 128: 607-619.

[26] Bányász Á. Gustavsson T. unpublished results.